Catalysis Letters 19 (1993) 143–151

# Nature of the active sites in H-ZSM-11 zeolite modified with Zn(2+) and Ga(3+)

Oscar A. Anunziata and Liliana B. Pierella

*Centro de Investigaciones Tecnologicas, GRUCOM, Facultad Regional Cordoba,*
*Universidad Tecnologica Nacional, C. C. 36 Suc. 16, 5016 Cordoba, Argentina*

Received 13 December 1992; accepted 2 April 1993

H-ZSM-11 zeolite modified with zinc and gallium by ion exchange was investigated using XRD, IR and TPD of ammonia. The modification of the material by zinc produced a lowering of the strong Brønsted acidic sites generating new and strong Lewis sites. Unlike zinc-zeolites, the gallium is localized preferentially on the outer surface of microcrystallites blocking a few Brønsted centers.

**Keywords:** Zeolites; Zn-ZSM-11; Ga-ZSM-11; active centres; XRD; IR; TPAD

## 1. Introduction

ZSM-5 and ZSM-11 zeolites are currently of particular interest for aromatization of light paraffins. Modifications of zeolites with zinc or gallium have been successfully used for this purpose [1–5]. Many papers are devoted to study of the mechanism of activation and aromatization of lower alkanes over these catalysts [1,3,4,6–9]. Recent work [10,11] showed that zinc is localized as a counter ion and that the position of gallium is dependent on the activation treatment [12,13]. The present paper contributes to the knowledge of the nature of active centers of zinc and gallium modified zeolites. Results from X-ray powder diffraction (XRD), infrared spectroscopy (IR) and temperature programmed desorption (TPD) allowed us to obtain important conclusions.

## 2. Experimental

### 2.1. MATERIALS

ZSM-11 zeolites (Si/Al = 17) were obtained by hydrothermal crystallization in the $Na_2O$–$Al_2O_3$–$SiO_2$ system, using tetrabutylammonium hydroxide as a structure directing agent by known methods [14] with some modifications [15]. The $NH_4^+$-form of zeolites was prepared by ion-exchange with $NH_4Cl$ 1 M (30 ml/g catalyst) by twice refluxing it for 20 h. Zn and Ga zeolites were obtained by ion-exchange of $NH_4^+$-zeolite with zinc or gallium nitrate solutions (0.05 M, 80°C for 4–30 h). The samples were washed with water and dried for 10 h at 100°C in air.

The samples investigated in this study are denoted as: $NH_4^+$-ZSM-11 **1**, H-ZSM-11 **2**, 0.46$NH_4^+$0.54Zn-ZSM-11 **3**, 0.16$NH_4^+$0.84Zn-ZSM-11 **4**, 0.16H0.84Zn-ZSM-11 **5**, $NH_4^+$Ga-ZSM-11 **6**, HGa-ZSM-11 **7**. Samples **1**, **3**, **4** and **6** were employed for TPAD (temperature programmed ammonia desorption). Samples **2**, **5** and **7** were obtained after deammoniation of samples **1**, **4** and **6**, respectively and used for the IR and XRD studies. Samples **5** and **7** were analyzed by scanning electron microscopy (SEM), energy dispersive X-ray (EDX) and **5** by X-ray photoelectron spectroscopy XPS.

### 2.2. METHODOLOGY

Every sample showed good purity and crystallinity by XRD. TPAD experiments were carried out in a conventional TPD apparatus with a flame ionization detector. The spectra were obtained by raising the temperature at a rate of 10°C/min with a temperature programmable controller, under 20 ml/min flow of $N_2$. Infrared measurements were performed on a Nicolet 710 FTIR spectrometer. Samples were pressed into self-supporting wafers (8–10 mg $cm^{-2}$). The greaseless cell used for these studies is similar to the IR cell described previously [16]. Pyridine (3 Torr) was adsorbed at room temperature for a minimum of 2 h, and desorbed for 1 h at 250, 350 and 400°C at $10^{-5}$ Torr.

## 3. Results and discussion

Table 1 reports the chemical composition of catalysts obtained by X-ray fluorescene (XRF) and atomic absorption (AA).

Table 1
Chemical composition (molar ratio) of the catalytic material

| Catalyst | Si/Al | Si/Na | Si/Zn | Si/Ga |
|---|---|---|---|---|
| Na-ZSM-11 | 17.30 | 15.20 | | |
| H-ZSM-11 2 | 17.25 | >5000 | | |
| H-Zn-ZSM-11 3 | 17.25 | >5000 | 118 | |
| H-Zn-ZSM-11 5[a] | 17.36 | >5000 | 68 | |
| H-Ga-ZSM-11 7 | 17.00 | >5000 | | 76.5 |

[a] XPS results (atomic ratio) Si/Al = 60.6; Al/Zn = 89; EDX data: Si/Al = 18.9; Al/Zn = 3.71.

### 3.1. X-RAY MEASUREMENTS

Samples of zeolites ZSM-11 **2** and **5** showed XRD patterns consistent with published results [14]. ZnO peak positions in the XRD pattern of sample **5** (35–37° $2\theta$) were not observed. Reflections due to ZnO and ZSM-11 were detected when H-ZSM-11 was modified by impregnation with zinc nitrate solution and calcined in air at 540°C. Reflections of ZSM-11 (23–24° $2\theta$) and $Ga_2O_3$ (35–36 and 39–39.8° $2\theta$) were observed in sample **7**. Additional experimental evidence about the distribution of zinc and gallium was found by SEM–EDX analysis. Crystal sizes were about 1–1.5 μm. EDX spectra of **5** showed emission at 0.83 and 8.79 keV corresponding to zinc present in the sample. Thus, the zinc was present as parallelepiped crystallites characteristic of ZSM-11 type zeolite. The zinc tended to distribute uniformly in zeolite crystallites. Unlike Zn-zeolites, the gallium can be seen only as an individual formation located on the outer surface of the zeolites for sample **7**. XPS data of **5** indicated that zinc was not incorporated on the outer surface of zeolite crystallites (table 1).

### 3.2. TPAD MEASUREMENTS

Fig. 1 shows results of TPAD experiments obtained for ZSM-11 samples **1**, **3**, **4** and **6**. Thermal desorption of ammonia occurred in two stages when ammonia was sorbed on H-ZSM-5 and ZSM-11. Water and ammonia were the detected products. In this work, since ammonia was not sorbed, the ammonia recorded by TPAD analysis can only be obtained by a thermal deammoniation process on ammonium-zeolites. In the same way, using an FID detector, water molecules

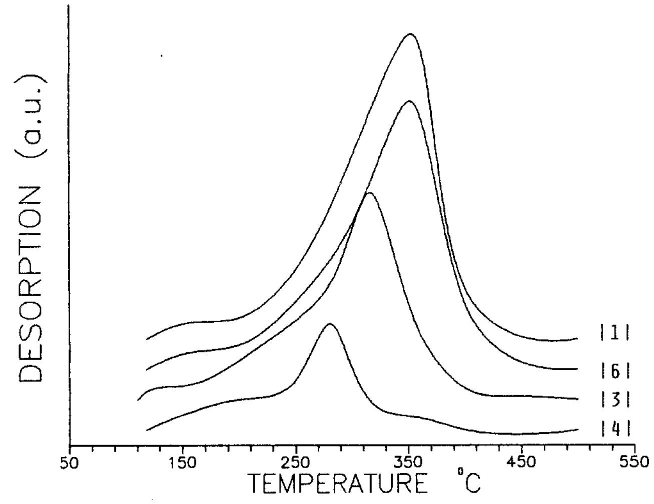

FIGURE 1

Fig. 1. Temperature programmed ammonia desorption from samples **1**, **3**, **4** and **6**.

cannot be registered and only the high temperature peak (h-peak) appeared [17] (fig. 1). According to literature data, the h-peak indicates the interaction of ammonia with Brønsted acidic sites [18]. TPAD spectra of **1** and **6** were not quite different, but an h-peak of **6** was a little smaller than of sample **1** (fig. 1a). Sample **4** showed the h-peak shifted to lower temperature and was smaller than the h-peak for sample **1**. These experimental facts can be explained as follows. The ion-exchange process which does not lead to a complete exchange of ammonium for zinc, as detected by thermal deammoniation experiments, suggests that the remaining protons have low acidic strength. Thus, zinc ions were incorporated as counter ions that initially block strong Brønsted acidic sites. Knai [19] found that the highest temperature peak shifted to low temperature and was smaller than that of H-ZSM-5 in TPD experiments of ammonia preadsorbed on Ga-ZSM-5. Besides, the peak intensity decreased as the pretreatment temperature was increased from 540 to 780°C, although this was not observed here. TPAD results obtained for Zn-zeolite and Ga-zeolite are novel data that show differences between zinc and gallium incorporation. Zinc ions introduced in ZSM-11 zeolite by ammonium exchange decreased the concentration of the strongest Brønsted acidic sites [10] by blocking negatively charged tetrahedral $AlO_4$ groups. In Ga loaded zeolites, the gallium was localized on the outer surface of crystallites without interaction with OH groups. $Ga_2O_3$ reduced at high temperature initially produced a surface migration and later an interaction between acidic OH groups and reduced gallium oxide [12].

## 3.3. IR SPECTROSCOPIC STUDIES

### *3.3.1. Structural hydroxyl groups*

Figs. 2a, 3a and 4a show the spectra of samples **2**, **5** and **7**, respectively in the 3900–3300 $cm^{-1}$ range. Samples **2** and **7** exhibited IR bands at 3610, 3690–3685 and 3740 $cm^{-1}$ indicating the presence of some irregularities in the lattice. Bands at 3500 and 3725 $cm^{-1}$ (free hydroxyl groups caused by dealumination) were absent, indicating, according to Jentys et al. [20], that extra-lattice species, i.e. alumina, was not present. The IR bands at 3610 and 3740 $cm^{-1}$ can be assigned to Brønsted acidic sites [Si(OH)Al] and terminal Si–OH groups, respectively. According to Datka and Tuznik [12], OH groups of H-ZSM-5 at 3738–3740 $cm^{-1}$ are not acidic enough to react with pyridine. Some of these OH groups are situated on the external faces of crystallites and the others are inside the channels. The amount of silanol groups for H-ZSM-11 is about twice as high as in H-ZSM-5 type zeolite [22] as our experimental IR data showed. The introduction of zinc decreased the intensity of the 3610 $cm^{-1}$ band in sample **5**. Otherwise, no additional bands could be seen that might be assigned to OH groups attached to $Zn^{2+}$. The IR vibration of [Si(OH)Al] groups at 3610 $cm^{-1}$ was affected in a different way for sample **7**. It was lightly attenuated, but a new absorption at 3660 $cm^{-1}$ appeared. Ga-modified zeolite, **7**, exhibited four different bands at 3610, 3660, 3690 and 3740 $cm^{-1}$. A new absorption at 3660 $cm^{-1}$ is difficult to assign at present. Kasansky et al. [23]

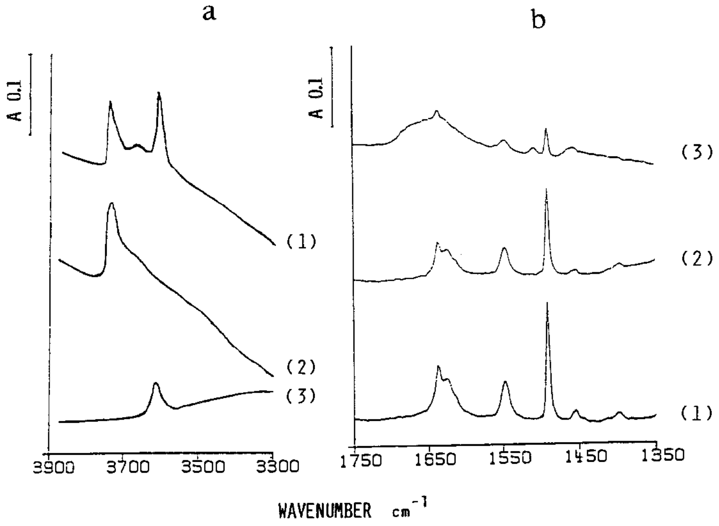

Fig. 2. (a) IR spectra of OH groups in sample **2**; (1): zeolite heated in vacuo ($10^{-5}$ Torr) at 400°C; (2): (1) plus pyridine adsorbed at room temperature and outgassed at 250°C and $10^{-5}$ Torr; (3): (1) – (2) difference spectrum. (b) Typical IR bands in the 1350–1750 cm$^{-1}$ region for pyridine adsorbed at room temperature and outgassed at (1) 50, (2) 350, (3) 400°C at $10^{-5}$ Torr for sample **2**.

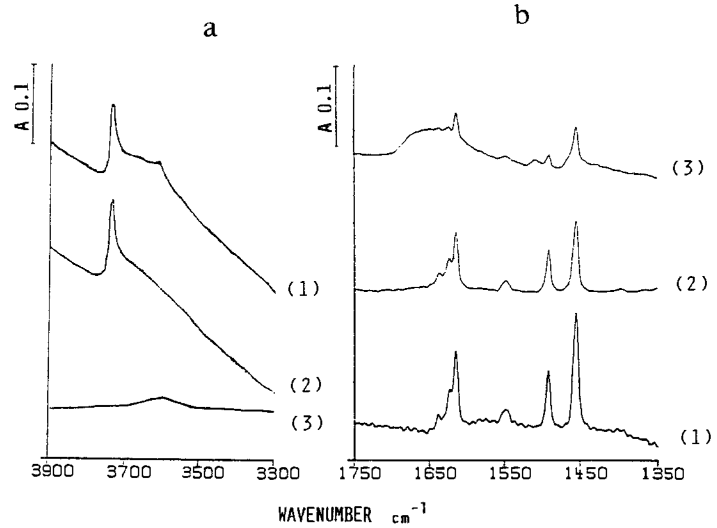

Fig. 3. (a) IR spectrum of OH groups in sample 5; (1): zeolite heated in vacuo ($10^{-5}$ Torr) at 400°C; (2): (1) plus pyridine adsorbed at room temperature and outgassed at 250°C and $10^{-5}$ Torr; (3): (1) – (2) difference spectrum. (b) Typical IR bands in the 1350–1750 cm$^{-1}$ region for pyridine adsorbed at room temperature and outgassed at (1) 250, (2) 350, (3) 400°C at $10^{-5}$ Torr for sample 5.

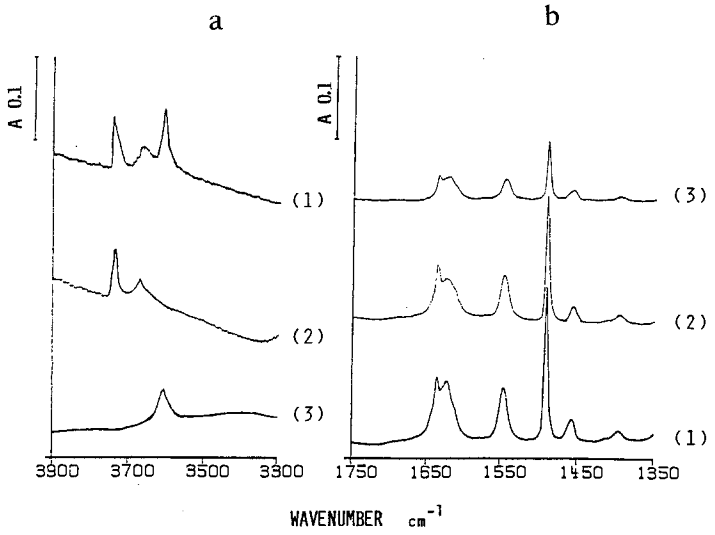

Fig. 4. (a) IR spectra of OH groups in sample **7**; (1): zeolite heated in vacuo ($10^{-5}$ Torr) at 400°C; (2): (1) plus pyridine adsorbed at room temperature and outgassed at 250°C and $10^{-5}$ Torr; (3): (1) – (2) difference spectrum. (b) Typical IR bands in the 1350–1750 $cm^{-1}$ region for pyridine adsorbed at room temperature and outgassed at (1) 250, (2) 350, (3) 400°C at $10^{-5}$ Torr for sample **7**.

observed this absorption band in ZnO-zeolites and attributed it to a Zn–OH interaction. Meriaudeau and Naccache [12] related the 3660 $cm^{-1}$ band to the presence of an OH group on gallium oxide or $Ga^{x+}$ ions.

### *3.3.2. Adsorption and desorption of pyridine*

Infrared spectra of pyridine adsorbed on acidic catalysts have often been used for characterizing the nature and strength of acidic sites in H-ZSM-5 zeolites [24]. Figs. 2b, 3b and 4b show IR spectra for chemisorbed pyridine after adsorption at room temperature and after further outgassing the samples **2**, **5** and **7** at 250, 350 and 400°C. Absorption bands due to chemisorbed pyridine at 1450–1460, 1490–1495, 1545–1550, 1620–1630, 1640–1645 $cm^{-1}$ are observed. Bands at 1450 and 1550 $cm^{-1}$ indicated the presence of both Lewis and Brønsted acidic sites [24]. The strong absorption band at 1613 $cm^{-1}$ in sample **5** indicated Lewis acidic sites and will be discussed elsewhere [25]. The number of Lewis sites increased as Brønsted sites decreased upon introduction of zinc. Furthermore, new Lewis sites were very strong since they retain more pyridine than the parent H-ZSM-11 material after outgassing at 400°C.

### *3.3.3. Concentration and strength of acidic sites*

A careful analysis of IR data (figs. 2b, 3b and 4b), allowed us to determine the concentration of Brønsted-acidic sites and Lewis-acidic sites. The concentration of pyridine interacting with Brønsted acidic sites, $PyH^+$ was calculated from the maximum intensity of the absorption at 1545 $cm^{-1}$. Fig. 5 reports the relative absorbances of the IR band expressed per mg of zeolite as a function of outgassing temperatures for $PyH^+$. We calculated the concentration of the Lewis-acidic sites by using the intensity of band at 1450–1460 $cm^{-1}$. That absorption indicated the electron-donor–acceptor adduct EDA, of pyridine-Lewis sites in zeolites. To study the strength of Brønsted and Lewis acidic sites we arbitrarily defined three different values, weak (w), medium (m) and strong (s) acidic sites as they still hold pyridine after desorption at 250, 350 and 400°C, respectively. Results obtained for PyL can be seen in fig. 6. From the results shown in figs. 5 and 6 we concluded that after modification of the zeolite by zinc, the $Zn^{2+}$ ions were exchanged with strongly acidic sites (3610 $cm^{-1}$ IR band). New and stronger Lewis-acidic sites were created after zinc loading since pyridine was retained after desorption at 400°C. The weak signal at 1545 $cm^{-1}$ for adsorbed pyridine indicates that the active sites in zinc loaded zeolites produced a catalyst with stronger Lewis acidic sites than Brønsted sites. The ratio of Lewis sites/Brønsted sites would be a function of ion-exchange capacities. Further results about this conclusion can be obtained elsewhere [26,27]. According to data shown in figs. 5 and 6, Brønsted sites in the Ga-zeolite were only slightly loaded with gallium. This fact can be explained by the large size of $Ga^{3+}$ ion and the low probability for compensation of three negative charges on the zeolite framework [10,23]. The small increase in concentration of Lewis acidic sites indicates that the incorporated gallium has a low interaction with pyridine through an EDA complex.

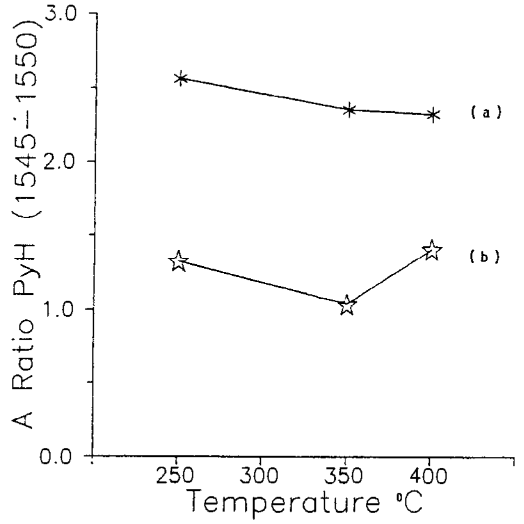

Fig. 5. The dependence of absorbance of pyridine adsorbed to Brønsted acidic sites (1545–1550 $cm^{-1}$) as a function of outgassing temperature: absorbance ratio per mg sample (a) $A(2)/A(5)$; (b) $A(2)/A(7)$.

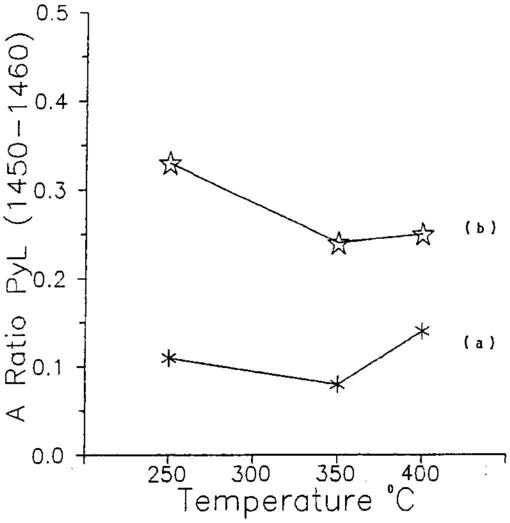

Fig. 6. The dependence of absorbance of pyridine adsorbed to Lewis acidic sites (1450–1460 $cm^{-1}$) as a function of outgassing temperature: absorbance ratio per mg sample (a) $A(2)/A(5)$; (b) $A(2)/A(7)$.

## 4. Conclusions

XRD, TPAD and pyridine IR results, allowed us to better understand structural and catalytic features of zinc and gallium ion-exchanged loaded zeolites.

Zinc and gallium distributions in treated zeolites are quite different. Zn tended to distribute itself uniformly in zeolite channels interacting with Brønsted acidic sites and produced new and stronger Lewis sites. On the other hand, Ga did not penetrate the zeolite channels and was located as individual oxide particles on the outer surface of the material. Nevertheless sone of the gallium interacted with a few Brønsted sites by migration within the zeolite when temperature pretreatments in oxygen/hydrogen atmosphere were carried out [12,13]. In zinc loaded zeolites only Lewis acidic sites with high strength were obtained when the zinc content increased. Brønsted acidic sites were weak or medium strength. On the other hand, Ga-zeolites produced stronger Brønsted centers, although in lower concentrations than those of H-ZSM-11 zeolites. These results renew an interest in understanding the mechanism of aromatization of lower alkanes over zinc and gallium modified zeolites.

## Acknowledgement

The present work was partially supported by a grant from CONICET Argentina-

PID 3-08220/89. We thank Dr. Vicente Fornes, Instituto de Tecnologia Química, Universidad Politecnica de Valencia, Spain, for performing the IR experiments and for many stimulating discussions.

## References

[1] T. Mole, J.R. Anderson and G. Creer, Appl. Catal. 17 (1985) 141.
[2] H. Kitagawa, Y. Sendoda and Y. Ono, J. Catal. 101 (1986) 12.
[3] Y. Ono, H. Kitagawa and Y. Sendoda, Sekiyu Gakkaishi (J. Japan. Petroleum Inst.) 30 (1987) 77.
[4] O.A. Anunziata, O.A. Orio, L.B. Pierella and M.C. Aguirre, React. Kinet. Catal. Lett. 39 (1989) 75.
[5] O.A. Anunziata, L.B. Pierella and O.A. Orio, React. Kinet. Catal. Lett. 43 (1991) 67.
[6] P. Meriaudeau and C. Naccache, J. Mol. Catal. 59 (1990) L31.
[7] C.R. Bayense, A.J.H.P. van der Pol and J.H.C. van Hooff, Appl. Catal. 72 (1991) 81.
[8] G. Buckles, G.J. Hutchings and C.D. Williams, Catal. Lett. 11 (1991) 89.
[9] P. Meriaudeau and C. Naccache, in: *Zeolite Chemistry and Catalysis*, Studies in Surface Science and Catalysis, Vol. 69, eds. P.A. Jacobs, N.I. Jaeger, L. Kubelková and B. Wichterlová (Elsevier, Amsterdam, 1991) p. 405.
[10] V.M. Yakerson, T.V. Vasina, L.I. Lafer, V.P. Syntnyk, G.L. Dykh, A.V. Mokhov, O.V. Bragin and Kh.M. Minachev, Catal. Lett. 3 (1989) 339.
[11] L.M. Kustov, V.B. Kazansky, S.G. Hegde, K.R. Kamble and P. Ratnasamy, Indian J. Chem. 29 (1990) 101.
[12] P. Meriaudeau and C. Naccache, Appl. Catal. 73 (1991) L13.
[13] V. Kanazirev, G.L. Price and K.M. Dooley, in: *Zeolite Chemistry and Catalysis*, Studies in Surface Science and Catalysis, Vol. 69, eds. P.A. Jacobs, N.I. Jaeger, L. Kubelková and B. Wichterlová (Elsevier Amsterdam, 1991) p. 277.
[14] P. Chu, US Patent 3.709.979 (1972).
[15] O.A. Anunziata, Doctoral Thesis, Universidad Nacional de Cordoba, Argentina (1987).
[16] A. Aucejo, M.C. Burguet, A. Corma and V. Cortes, Appl. Catal. 22 (1986) 187.
[17] W. Reschetilowski, B. Unger and K.P. Wendlandt, J. Chem. Soc. Faraday Trans. I 85 (1989) 2941.
[18] L.M. Parker, D.M. Bibby and R.H. Meinhold, Zeolites 5 (1985) 384.
[19] J. Knai, in: *Successful Design of Catalysts*, ed. T. Inui (1988) 211.
[20] A. Jentys, G. Rumplmyk and J. Lercher, Appl. Catal. 25 (1989) 299.
[21] J. Datka and F. Tuznik, Zeolites 5 (1985) 230.
[22] J. Datka and Z. Piwowarska, Zeolites 8 (1988) 30.
[23] V.B. Kazansky, L.M. Kustov and A.Yu. Khodakov, in: *Zeolites: Facts, Figures, Future*, Studies in Surface Science and Catalysis, Vol. 49, eds. P.A. Jacobs and R.A. van Santen (Elsevier, Amsterdam, 1989) p. 1173.
[24] J.C. Vedrine, A. Auroux, V. Bolis, P. Dejaifve, C. Naccache, P. Wierzchowski, E. Derouane, J. Nagy, J.P. Gilson, J.H.C. van Hooff, J.P. van den Berg and J. Wolthuizen, J. Catal. 59 (1979) 248.
[25] O.A. Anunziata and L.B. Pierella, to be published.
[26] O.A. Anunziata and L.B. Pierella, Catal. Lett. 16 (1992) 437.
[27] O.A. Anunziata, L.B. Pierella and H.R. Macaño, to be published.